applied optics

Accurate estimate and measurement of continuous-wave noise in filtered incoherent light

Marko Šprem* and Dubravko Babić

University of Zagreb, Faculty of Electrical Engineering and Computing, Unska 3, 10000 Zagreb, Croatia
*Corresponding author: marko.sprem@fer.hr

Received 1 September 2016; revised 25 January 2017; accepted 26 January 2017; posted 30 January 2017 (Doc. ID 274958); published 17 February 2017

We derive an exact expression for the continuous-wave signal-to-noise ratio of filtered incoherent light, which applies to arbitrary optical filtering and arbitrary receiver electrical response. We demonstrate a simple method for making accurate measurements of continuous-wave signal-to-noise ratio, and compare these measurements with values computed from independent measurements of optical-filter coherence time and receiver electrical response; our measurements and computed values agree to within ±0.2 dB.

OCIS codes: (030.6600) Statistical optics; (060.2330) Fiber optics communications.

https://doi.org/10.1364/AO.56.001724

1. INTRODUCTION

The noise in photoelectric mixing of incoherent light has been a subject of interest for a long time in spectroscopy [1,2], imaging optics [3], fiber-optic amplifiers [4], and communication systems based on spectrum slicing [5–7]. The signal-to-noise ratio (*SNR*) of filtered incoherent light measured using a photodetector with response time τ_D in comparison with the coherence time τ_C of the optical beam is given by [8]

$$SNR = \frac{\langle i(t)\rangle^2}{\mathrm{var}(i(t))} = \frac{1}{\langle g^{(2)}(0)\rangle_D - 1} = \frac{\tau_D}{\tau_C}, \tag{1}$$

where $i(t)$ is the time-dependent detector current, $\langle i(t)\rangle$ and $\mathrm{var}(i(t))$ are the expected value and variance of that current, and $\langle g^{(2)}(0)\rangle_D$ is the second-order degree of coherence of the light beam averaged over the response time of the detector.

The analysis leading to Eq. (1) has been revisited in optical communications employing spectrum-sliced spontaneous emission [5,6,9], where the excess noise was estimated for incoherent light filtered with a variety of optical filter and receiver electrical bandwidth shapes, all under the same assumption: that the measurement time is much longer than the coherence time of the optical source. The resulting expression for *SNR*, consolidated from Refs. [6,7,10,11], and corrected for an arbitrary degree of coherence [3], can be written as

$$SNR \approx \left(\frac{2}{1+P^2}\right)\cdot\frac{1}{2B_E\tau_C}, \tag{2}$$

where B_E is the equivalent noise bandwidth (ENB) of the receiver (in Hertz), τ_C the optical coherence time, and P the degree of polarization. The ENB B_E of the receiver is defined as

$$B_E = \frac{\int_0^\infty |H(f)|^2 \mathrm{d}f}{|H(0)|^2}, \tag{3}$$

where $H(f)$ is the electrical transfer function of the receiver. The coherence time τ_C, commonly expressed with optical bandwidth $B_O = 1/\tau_C$, can be computed from the optical-signal electric-field autocorrelation $R_O(\tau)$ [3] or, equivalently, from the double-sided power-spectral density $S(\omega)$ of the optical field [7,10]:

$$\tau_C = \int_{-\infty}^{\infty}\left|\frac{R_O(\tau)}{R_O(0)}\right|^2 \mathrm{d}\tau = 2\pi\frac{\int_{-\infty}^{\infty}|S(\omega)|^2\mathrm{d}\omega}{\left(\int_{-\infty}^{\infty}S(\omega)\mathrm{d}\omega\right)^2}. \tag{4}$$

The degree of polarization P is defined as the ratio of optical powers of the polarized fraction to the total power in the optical beam [3]. Note that incoherent unpolarized light exhibits a larger *SNR* relative to polarized light for the same $2B_E\tau_C$. The $2/(1+P^2)$ term originates from combining two uncorrelated and incoherent light beams with varying degrees of polarization [3].

The essential condition for the validity of Eq. (2) is that the optical filter bandwidth B_O is much greater than the electrical filter bandwidth B_E, namely, Eq. (2) is valid for large *SNR* values ($SNR \gg 1$). We state this condition as

$$2B_E\tau_C \ll 1. \tag{5}$$

Equation (2) has been used for estimating spontaneous-spontaneous emission beat noise in spectrum-sliced wavelength division multiplexed (WDM) communication systems [5,12] and its impact on the bit-error-rate (BER) [13]. The key feature of Eq. (2) is that *SNR* is independent of light intensity and hence places an ultimate limit on link performance [5,6].

In most applications, the condition in Eq. (5) applies and the abovementioned Eq. (2) is sufficient for estimating the *SNR* of filtered incoherent light. As a consequence, the focus of previous reports has been on deriving expressions for coherence times [Eq. (4)] for specific optical channels, for example, Lorentz and Gaussian channels [10,11,14], combined with various electrical filters, such as integrate-and-dump receivers [3,10].

What has not been addressed is the range of validity of Eq. (2) and how to compute the *SNR* for arbitrary optical and electrical bandwidth characteristics when the condition in Eq. (5) has not been met. To answer this question, in Section 2, we provide a generalization of Eq. (2) that is exact for arbitrary optical and electrical characteristics. We then estimate the error in *SNR* resulting from using Eq. (2) rather than the generalized form for Gaussian and Lorentz line shapes. In Section 3, we derive this generalized expression, while in Section 4, we describe a simple measurement of continuous-wave noise and signal-to-noise ratio and show that the measured values of *SNR* match those computed from known optical and electrical characteristics to within ±0.2 dB.

2. ARBITRARY OPTICAL AND ELECTRICAL FILTERS

For arbitrary optical power spectral density $S(\omega)$ and arbitrary electrical filter transfer function $H(\omega)$, the signal-to-noise ratio of incoherent light is given by

$$\frac{1}{SNR}=\left(\frac{1+P^2}{2}\right)\cdot\int_{-\infty}^{\infty}\frac{R_E(\tau)}{H^2(0)}\left|\frac{R_O(\tau)}{R_O(0)}\right|^2 \mathrm{d}\tau. \tag{6}$$

Here, $R_E(\tau)$ is the autocorrelation of the electrical filter and $R_O(\tau)$ the electric-field autocorrelation of the optical filter. The integral kernel is rather intuitive: it comprises a product of two functions, one of which contains the properties of the electrical filter, and the other the properties of the optical filter. When Eq. (5) is applied to Eq. (6), $R_O(\tau)$ becomes much sharper than $R_E(\tau)$ and effectively extracts $R_E(0)$ to the front of the integral and makes Eq. (6) converge to Eq. (2). In the other limit, when $2B_E\tau_C \gg 1$, $R_E(\tau)$ becomes sharp relative to $R_O(\tau)$ and the integral converges to unity resulting in $SNR=(1+P^2)/2$ as expected [3].

We use Eq. (6) to determine the range of validity of Eq. (2) for Gaussian and Lorentzian line shapes combined with a Gaussian electrical filter. We select a Gaussian electrical filter because of its similarity to Bessel filters, which are used in optical communications [15] due to their maximally flat group-delay characteristics.

The transfer function and autocorrelation of a Gaussian receiver with noise bandwidth B_E is given by

$$\begin{aligned}|H(\omega)|^2&=\exp\left(-\frac{\pi f^2}{4B_E^2}\right),\\ \frac{R_E(\tau)}{|H(0)|^2}&=2B_E\exp(-4\pi B_E^2\tau^2).\end{aligned} \tag{7}$$

For a Gaussian line shape, we obtain optical power spectral density (PSD) and associated normalized autocorrelation function as

$$S(\omega)=\exp\left(-\frac{\omega^2\tau_C^2}{2\pi}\right),\quad \left|\frac{R_O(\tau)}{R_O(0)}\right|^2=\exp\left(-\pi\frac{\tau^2}{\tau_C^2}\right). \tag{8}$$

By inserting Eqs. (7) and (8) into Eq. (6) and integrating, we find the *SNR* to be

$$\frac{1}{SNR}=\left(\frac{1+P^2}{2}\right)\frac{2B_E\tau_C}{\sqrt{1+(2B_E\tau_C)^2}}. \tag{9}$$

From here we see that Eq. (2) underestimates the *SNR* when $2B_E\tau_C$ becomes large. For example, when $2B_E\tau_C \geq 3/4$, *SNR* will be underestimated by at least 20% (1 dB) when using Eq. (2) rather than Eq. (9).

For the Lorentzian line shape, we define optical PSD and associated square of the normalized autocorrelation function as

$$S(\omega)=\frac{1}{1+(\omega\tau_C)^2},\quad \left|\frac{R_O(\tau)}{R_O(0)}\right|^2=\exp\left(-\frac{2|\tau|}{\tau_C}\right). \tag{10}$$

Inserting Eqs. (7) and (10) into Eq. (6) and integrating, we obtain

$$\frac{1}{SNR}=\left(\frac{1+P^2}{2}\right)\cdot\exp\left(\frac{1}{\pi\cdot(2B_E\tau_C)^2}\right)\cdot\operatorname{erfc}\left(\frac{1}{\sqrt{\pi}\cdot 2B_E\tau_C}\right). \tag{11}$$

From here we find that for $2B_E\tau_C \geq 1/2$, the *SNR* is underestimated by 20% (1 dB) if one uses Eq. (2) rather than Eq. (11). The Lorentz line shape error is larger for a given $2B_E\tau_C$ value because the autocorrelation in Eq. (10) is sharper than in Eq. (8) and makes the integral in Eq. (6) more sensitive to the rate of electrical filter autocorrelation spreading. The above estimates of *SNR* illustrate that the accuracy of Eq. (2) depends on the actual shape of the optical and electrical transfer functions, namely, that knowing the product $2B_E\tau_C$ is not sufficient for accurate estimate of the *SNR* when the condition in Eq. (5) no longer holds.

In spectrum-sliced systems and other applications where incoherent light is filtered, the PSD is determined by the array-waveguide grating, which comes with a variety of transmission spectra (see examples in Fig. 4). In this case, rather than obtaining the *SNR* analytically (as shown above), one should measure the optical filter transmission and the receiver transfer function, and then numerically perform the integration in Eq. (6) to obtain the expected *SNR*.

In the next section, we derive Eq. (6), while in last section of this work, we demonstrate that measuring the optical filter and the electrical characteristics of the receiver can be used to accurately estimate the signal-to-noise ratio of filtered incoherent light using a simple method for continuous-wave *SNR* measurement.

3. DERIVATION OF EQUATION (6)

We study the optical signal-to-noise ratio (*SNR*) given by [3]:

$$SNR=\left(\frac{2}{1+P^2}\right)\cdot\frac{\langle W\rangle^2}{\sigma_W^2}, \tag{12}$$

where $\langle W\rangle$ is the filtered sample of expected light intensity $\langle I\rangle$ and σ_W is the associated noise power measured in the detector current (detector responsivity is calibrated out; explained in

later text). Light intensity is treated as a wide-sense stationary stochastic process [16]. Relating *SNR* to bit-error rate (BER) requires knowing the intensity noise probability density function [17,18]. In Ref. [3], Goodman presented a filtered thermal-light treatment that was applicable to an arbitrary optical filter and an integrate-and-dump receiver (rectangular temporal measurement window). Following Goodman [3], we derive $\langle W\rangle$ and $\langle W^2\rangle$ as functions of the optical and electrical filter characteristics:

$$\begin{aligned}\langle W\rangle &= \lim_{A\to\infty}\frac{1}{A}\int_{-A/2}^{A/2}\mathrm{d}t\int_{-\infty}^{\infty}h(\xi-t)I(\xi)\mathrm{d}\xi\\ &= \int_{-\infty}^{\infty}h(x)\left\{\lim_{A\to\infty}\frac{1}{A}\int_{-A/2}^{A/2}I(x+t)\mathrm{d}t\right\}\mathrm{d}x\\ &= \langle I\rangle\cdot\int_{-\infty}^{\infty}h(x)\mathrm{d}x = \langle I\rangle\cdot H(0).\end{aligned}\tag{13}$$

Here, $H(\omega)$ is the Fourier transform of the electrical-filter impulse response $h(t)$. To obtain the variance, we find the expected value of W^2 by integrating the fluctuations over a long period of time:

$$\langle W^2\rangle = \lim_{A\to\infty}\frac{1}{A}\int_{-A/2}^{A/2}\int_{-\infty}^{\infty}\int_{-\infty}^{\infty}h(\eta-t)h(\xi-t)I(\xi)I(\eta)\mathrm{d}\eta\mathrm{d}\xi.\tag{14}$$

Using the substitutions $\xi' = \xi - t$ and $\eta' = \eta - t$, Eq. (14) is converted to

$$\begin{aligned}\langle W^2\rangle = &\int_{-\infty}^{\infty}\int_{-\infty}^{\infty}h(\eta')h(\xi')\\ &\times\left\{\lim_{A\to\infty}\frac{1}{A}\int_{-A/2}^{A/2}I(t+\xi')I(t+\eta')\mathrm{d}t\right\}\mathrm{d}\eta'\mathrm{d}\xi',\end{aligned}\tag{15}$$

where we recognize the inner integral as an autocorrelation of the light intensity,

$$\begin{aligned}R_I(\xi'-\eta') &= \langle I(\xi')I(\eta')\rangle\\ &= \lim_{A\to\infty}\frac{1}{A}\int_{-A/2}^{A/2}I(t+\xi')I(t+\eta')\mathrm{d}t.\end{aligned}\tag{16}$$

Note that the beam intensity is a stationary stochastic process. The expected value $\langle W^2\rangle$ is now

$$\langle W^2\rangle = \int_{-\infty}^{\infty}\int_{-\infty}^{\infty}h(\eta')h(\xi')R_I(\xi'-\eta')\mathrm{d}\eta'\mathrm{d}\xi'.\tag{17}$$

Further simplification of the integral is obtained by recognizing that the h' terms will yield another autocorrelation if we introduce $\tau = \xi' - \eta'$. Setting

$$R_E(\tau) = \int_{-\infty}^{\infty}h(\eta'+\tau)h(\eta')\mathrm{d}\eta',\tag{18}$$

we finally obtain

$$\langle W^2\rangle = \int_{-\infty}^{\infty}R_E(\tau)R_I(\tau)\mathrm{d}\tau.\tag{19}$$

The autocorrelation of the electrical filter $R_E(\tau)$ is obtained in a straightforward fashion by measuring the frequency response $H(\omega)$ and applying Wiener–Khinchin theorem.

The autocorrelation of the intensity of the light beam is proportional to the degree of second-order coherence of light. For filtered incoherent light, the relationship between the first and second degree of coherence is given by [8]

$$g^{(2)}(\tau) = 1 + |g^{(1)}(\tau)|^2,\tag{20}$$

where $g^{(1)}(\tau)$ and $g^{(2)}(\tau)$ are the first and second orders of coherence, respectively. The degrees of coherence can be related to the autocorrelations of electromagnetic wave intensity $R_I(\tau)$ and electromagnetic field $R_O(\tau)$, via

$$g^{(1)}(\tau) = \frac{\langle E(t)E(t+\tau)\rangle}{\langle E^2\rangle} = \frac{R_O(\tau)}{R_O(0)},\tag{21}$$

$$g^{(2)}(\tau) = \frac{\langle I(t)I(t+\tau)\rangle}{\langle I\rangle^2} = \frac{H^2(0)}{\langle W\rangle^2}R_I(\tau).\tag{22}$$

Combining Eqs. (20)–(22) we obtain the optical intensity autocorrelation,

$$R_I(\tau) = \frac{\langle W\rangle^2}{H^2(0)}\left\{1+\left|\frac{R_O(\tau)}{R_O(0)}\right|^2\right\}.\tag{23}$$

Inserting Eq. (23) into Eq. (19) and then combining Eqs. (13) and (12), we arrive at Eq. (6): a general relation for continuous-wave signal-to-noise ratio as a function of arbitrary optical and electrical filter transfer functions, and degree of polarization that does not require the assumption in Eq. (5). This is not the only way to derive Eq. (6). For example, one can arrive at Eq. (6) from the intermediate step (25) of reference [10] by performing two integrations and applying the Wiener–Khinchin theorem.

4. MEASUREMENT RESULTS

With the limits of Eq. (2) outlined, our goal is to show that *SNR* values computed from measured optical and electrical transfer functions can, with reasonable certainty, be used to estimate the actual *SNR*; our data experiments show to within ±0.2 dB. To this end, we developed a simple measurement method for making accurate *SNR* measurements on continuous-wave optical signals.

Measurement of noise and signal-to-noise ratio of filtered incoherent light has been performed using an oscilloscope [7,14], RF spectrum analyzer [6,11,13,19], and evaluated from bit-error rate [17]. We base our continuous-wave noise measurement on the RIN_XOMA measurement approach from a 10-Gb Ethernet standard [15] which we adapt for continuous-wave measurement by using a separate optical power meter for the average optical power in addition to the RF power meter for the noise. The setup is illustrated in Fig. 1(a). As the source of incoherent light we use an unpolarized broadband light source (BLS) which emits amplified spontaneous emission from an erbium-doped fiber amplifier with an emission spectrum centered at 1550 nm and a 30-nm bandwidth.

The BLS output is first passed through a variable optical attenuator and then through an isolator before it is fed to one of the channels of an arrayed waveguide grating (AWG). The filtered signal is split on a coupler with nominal coupling ratio $C_{12} = C_{14} = 50\%$, with port 2 coupled to an optical detector with AC-coupled voltage output and port 4 to a calibrated optical power meter. The fluctuations in the optical signal, converted to electrical noise, are filtered using an electrical

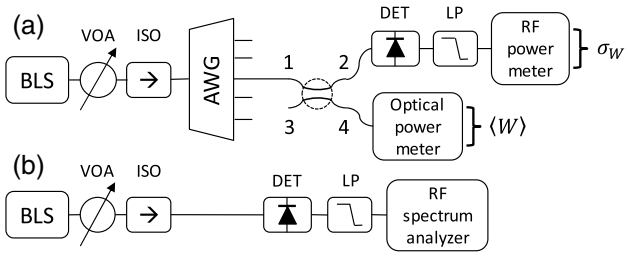

Fig. 1. Characterization setups for (a) the *SNR* measurements and (b) evaluation of ENBs of electrical filters (VOA, variable optical attenuator; ISO, optical isolator; DET, optical detector; LP, electrical low-pass filter).

filter and fed to a high-bandwidth 26.5-GHz RF power meter. The power spectral density is normalized to its value at low frequency, as needed in Eq. (3). The *SNR* is then obtained through the ratio of input optical power and its noise fluctuations.

We relate the variance of the AC voltage to optical fluctuations through the optical-detector responsivity coefficient R, measured independently to be 1360 ± 30 [V/W] with termination impedance $Z_0 = 50\ \Omega$. The detector is AC coupled, and to accurately determine R relative to the optical power meter, we applied a 2-MHz square wave signal on both the optical detector and the optical power meter and then inferred the relative calibration from the average to peak-to-peak values ratio. The dominant source of error in our *SNR* results is the uncertainty in the value of the optical-detector responsivity. The power P_{RF} measured on the RF power meter is proportional to the sum of the optical signal variance σ_W^2 and the other noise sources in the signal path referenced to the input of the optical head (equivalent input noise is denoted with σ_{OE}^2): $P_{\mathrm{RF}} \sim \sigma_W^2 + \sigma_{\mathrm{OE}}^2$. To evaluate $\langle W \rangle$ and σ_W^2 simultaneously, we varied the incident optical power P_{opt} using a variable optical attenuator through a wide range to eliminate the effect of the noise of the receiver (as is common in BER measurements). We extract the *SNR* value from the saturated part of the curve shown in Fig. 2, where the receiver noise is negligible. Furthermore, from the slope of the *SNR* versus the P_{opt} curve shown in Fig. 2, we extracted the equivalent input noise to be $\sigma_{\mathrm{OE}} = -27.6$ dBm. We then used this σ_{OE}^2 value and the *SNR* value obtained from the saturated part of the curve shown in Fig. 2 to compute the expected shape of the entire relationship.

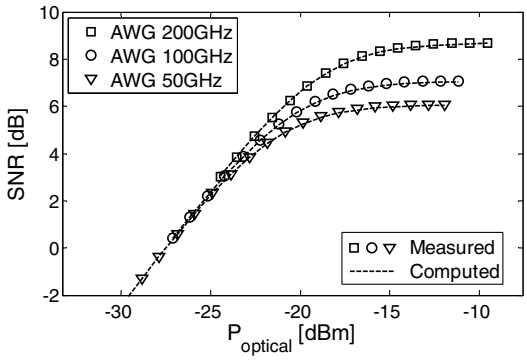

Fig. 2. Example of *SNR* measurement results for the unfiltered optical detector given for three different channel spacings.

This is shown along the measurement points noted as "computed" in Fig. 2. The excellent fit between shapes drawn by the measured and computed points implies that the optical noise of our receiver does not noticeably depend on intensity.

The accuracy of our noise measurement critically depends on the value of the responsivity which was accurately evaluated using the above-mentioned measurement. This difficulty could be alleviated if one were to use an optical head that is DC coupled. In this case, the responsivity would affect the noise and the average value of the light intensity equally.

We account for the difference in the coupling coefficients of the optical coupler splitting the average power and variance measurement. The accuracy of this coupling coefficient is important because any error $\Delta C/C$ alters the *SNR* by $2\Delta C/C$, as *SNR* is proportional to $C/(1-C)$. We calibrated the coupling coefficient C and also checked our results by making two measurements of *SNR*: one with the power meter connected to port 4 shown in Fig. 1(a), and another in which the coupler exit ports were exchanged. The geometric mean of the two obtained *SNR* values gives the correct *SNR* value that does not depend on the coupling coefficient or the loss in the optical coupler. For this method to work efficiently it is preferable that the coupling coefficient is around 50%, so that between the exchanges of the coupler ports, the *SNR* dependence on the equivalent input noise σ_{OE}^2 and the power at which saturation (in Fig. 2) occurs remain similar. The *SNR* values determined from the saturated levels in Fig. 2 are listed in Table 1, noted with "*M*".

We characterized four different electrical filters: the unfiltered optical detector with nominal 3.5-GHz bandwidth, and then the same optical head followed by fourth-order Bessel–Thompson filters with nominal 3-dB bandwidths equal to 940 MHz, 120 MHz, and 94 MHz. Bessel–Thompson filters are used because they have maximally flat group-delay. The ENBs of the filters were measured using the unfiltered BLS as a noise source and measuring the transmitted noise spectra on a spectrum analyzer, as shown in Fig. 1(b). The ENBs computed from the data shown in Fig. 3 are listed in Table 1.

We used three different athermal AWGs as optical filters, with channel separation of 200 GHz, 100 GHz and 50 GHz. We measured the optical transmission $S(\omega)$ through a select channel by connecting the BLS to the AWG common port (Fig. 4). The coherence time was then computed by numerically integrating the spectra. The results are listed in Table 1.

Table 1. Measurement Results for ENBs of Electrical Filters, Coherence Times of Optical Filters, and *SNR* Results Computed from Optical and Electrical Filter Characteristics (C) and from *SNR* Measurements (M); CS—Channel Separation

El. filter 3-dB [MHz]		94		120		940		3500	
B_E [MHz]		92.7		118		662		2863	
		SNR [dB]							
CS [GHz]	τ_C [ps]	C	M	C	M	C	M	C	M
200	5.78	32.7	32.9	31.7	31.8	24.2	24.5	17.8	17.8
100	12.5	29.3	29.4	28.3	28.3	20.8	21	14.4	14.5
50	19.6	27.4	27.4	26.4	26.3	18.9	19	12.5	12.6

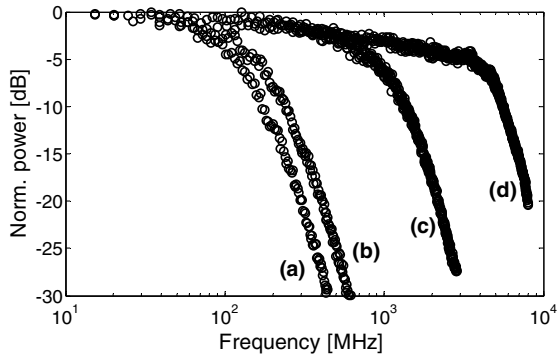

Fig. 3. Electrical filter transmission characteristics normalized to value at zero frequency: data (a)–(c) correspond to 94 MHz, 120 MHz, and 940 MHz low-pass filters inserted after the optical detector, respectively, while data (d) corresponds to the unfiltered optical detector.

Finally, we compute the *SNR* for all combinations of filters (three optical filters and four electrical filters) from their measured τ_C and B_E values. The degree of polarization P was kept at zero, inasmuch as the BLS was an unpolarized source. The computed *SNR* values are listed in Table 1, noted with "*C*". The results in Table 1 show that our method of estimating the *SNR* of incoherent light from accurately measuring the optical and electrical bandwidth indeed works well for all the tested filters and AWGs. The difference between measured and estimated value is at most 0.2 dB.

For all filter combinations listed in Table 1, we find that $2B_E\tau_C < 0.1$ and hence the correction achieved with using Eq. (6) rather than Eq. (2) is less than the measurement uncertainty. However, a combination of, for example, an array-waveguide grating with a 25-GHz channel separation and a 10-Gbps line rate with a receiver filter with $B_E \sim 7.5$ GHz, would result in $2B_E\tau_C \sim 0.6$ and a need to use Eq. (6) rather than Eq. (2).

As can be seen from the measurement results, the *SNR* improves with the increase of the optical filter bandwidth for incoherent light. This somewhat nonobvious phenomenon is expected and has been mathematically treated in multiple references [3,4,11,14]. All incoherent light components within the optical bandwidth B_O mix with each other during photodetection and their down-converted intermodulation products add at baseband, but only those components whose frequency falls within the electrical bandwidth B_E are detected. This detected baseband signal is hence a sum of approximately B_O/B_E signals with basically identical noise properties. Signal-to-noise ratio of a sum of noisy signals improves with the number of contributors because the variance of a sum of uncorrelated noisy signals increases with the number of those signals, while the square of the signal increases with the square of the number of contributors [16].

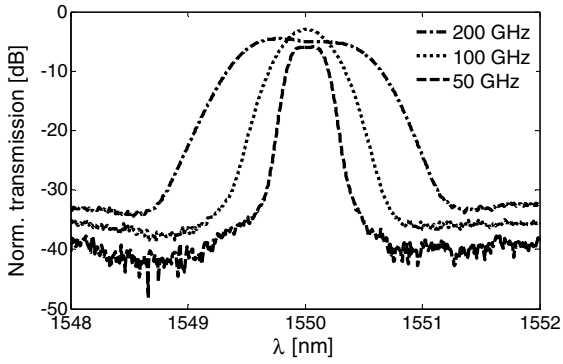

Fig. 4. Transmission spectra through one of the channels of each AWG with noted channel separation in gigahertz.

5. CONCLUSION

In conclusion, we derived an expression for the continuous-wave signal-to-noise ratio of filtered incoherent light which is exact for arbitrary optical and electrical filtering and degree of polarization. We used this expression to evaluate the range over which the conventional relationship Eq. (2) is valid. We furthermore confirmed experimentally that measuring the characteristics of the optical and electrical filters with sufficient accuracy can be used to accurately predict the *SNR* of incoherent light. To this end, we developed a simple method for measuring the *SNR*.

The importance of our general Eq. (6) lies with the fact that optical filters in WDM networks are becoming commensurate with the electrical filter bandwidths, and using the conventional $2B_E\tau_C \ll 1$ approximation to evaluate spontaneous-spontaneous emission beating noise is reaching the limits of its applicability.

Funding. Hrvatska Zaklada za Znanost (HRZZ) (IP-11-2013-3425).

REFERENCES

1. E. Gerjouy, A. T. Forrester, and W. E. Parkins, "Signal-to-noise ratio in photoelectrically observed beats," Phys. Rev. **73**, 922–923 (1948).
2. A. T. Forrester, R. A. Gudmundsen, and P. O. Johnson, "Photoelectric mixing of incoherent light," Phys. Rev. **99**, 1691–1700 (1955).
3. J. W. Goodman, *Statistical Optics* (Wiley, 1985).
4. N. A. Olsson, "Lightwave systems with optical amplifiers," J. Lightwave Technol. **7**, 1071–1082 (1989).
5. M. H. Reeve, A. R. Hunwicks, W. Zhao, S. G. Methley, L. Bickers, and S. Horning, "LED Spectral slicing for single-mode local loop applications," Electron. Lett. **24**, 389–390 (1988).
6. J.-S. Lee, Y. C. Chung, and D. J. DiGiovanni, "Spectrum-sliced fiber amplifier light source for multichannel WDM applications," IEEE Photon. Technol. Lett. **5**, 1458–1461 (1993).
7. G. J. Pendock and D. D. Sampson, "Transmission performance of high bit rate spectrum-sliced WDM systems," J. Lightwave Technol. **14**, 2141–2148 (1996).
8. R. Loudon, *The Quantum Theory of Light* (Oxford University, 1970).
9. E. Wong, K. L. Lee, and T. B. Anderson, "Directly modulated self-seeding reflective semiconductor optical amplifiers as colorless transmitters in wavelength division multiplexed passive optical networks," J. Lightwave Technol. **25**, 67–74 (2007).
10. J.-S. Lee, "Signal-to-noise ratio of spectrum-sliced incoherent light sources including optical modulation effects," J. Lightwave Technol. **14**, 2197–2201 (1996).
11. G.-H. Duan and E. Georgiev, "Non-white photodetection noise at the output of an optical amplifier: theory and experiment," IEEE J. Quantum Electron. **37**, 1008–1014 (2001).
12. C.-H. Lee, W. V. Sorin, and B. Y. Kim, "Fiber to the home using a PON infrastructure," J. Lightwave Technol. **24**, 4568–4583 (2006).
13. W. Chen, R. S. Tucker, X. Yi, W. Shieh, and J. S. Evans, "Optical signal-to-noise ratio monitoring using uncorrelated beat noise," IEEE Photon. Technol. Lett. **17**, 2484–2486 (2005).

14. G. Kweon and J. Choi, "Dependence of the signal-to-noise ratio for a mixture of coherent and incoherent sources on the incoherent source spectral profile," Opt. Rev. **10**, 185–195 (2003).
15. "Relative intensity noise optical modulation (RINxOMA) measuring procedure," IEEE Standard for Ethernet, IEEE Standard 802.3, Clause 52.9.6 (2015).
16. A. Papoulis, *Probability, Random Variables, and Stochastic Processes*, 2nd ed. (McGraw-Hill, 1984).
17. W. Mathlouthi, M. Menif, and L. A. Rusch, "Beat noise effects on spectrum-sliced WDM," Proc. SPIE **5260**, 44–54 (2003).
18. D. Marcuse, "Calculation of bit-error probability for a lightwave system with optical amplifiers and post-detection Gaussian noise," J. Lightwave Technol. **9**, 505–513 (1991).
19. A. D. McCoy, B. C. Thomsen, M. Ibsen, and D. J. Richardson, "Filtering effects in a spectrum-sliced WDM system using SO-based noise reduction," IEEE Photon. Technol. Lett. **16**, 680–682 (2004).